

## Polarization Studies of Resonant Forbidden Reflections in Liquid Crystals

P. Fernandes,<sup>1</sup> P. Barois,<sup>1</sup> S. T. Wang,<sup>2</sup> Z. Q. Liu,<sup>2</sup> B. K. McCoy,<sup>2</sup> C. C. Huang,<sup>2</sup> R. Pindak,<sup>3</sup> W. Caliebe,<sup>3</sup> and H. T. Nguyen<sup>1</sup>

<sup>1</sup>Université Bordeaux I, CNRS, Centre de Recherche Paul Pascal, Avenue A. Schweitzer, 33600 Pessac, France

<sup>2</sup>School of Physics and Astronomy, University of Minnesota, Minneapolis, Minnesota 55455, USA

<sup>3</sup>Brookhaven National Laboratory, National Synchrotron Light Source, Upton, New York 11973, USA

(Received 28 May 2007; published 26 November 2007)

We report the results of resonant x-ray diffraction experiments performed on thick films of a biaxial liquid crystal made of achiral bent-core molecules. Polarization properties of forbidden reflections are observed as a function of the sample rotation angle  $\varphi$  about the scattering vector  $\mathbf{Q}$  for the first time on a fluid material. The experimental data are successfully analyzed within a tensor structure factor model by taking the nonperfect alignment of the liquid crystal into account. The local structure of the  $B_2$  mesophase is hence determined to be  $\text{SmC}_S P_A$ .

DOI: 10.1103/PhysRevLett.99.227801

PACS numbers: 61.30.Eb, 61.10.Nz

Resonant (or anomalous) x-ray scattering occurs when the energy of the x-ray radiation approaches the values required to excite an inner-shell electron into an empty state of the outer shell or into a free electron state [1]. In such circumstances, the atomic scattering factor  $f_a$  exhibits a complex frequency-dependent contribution in addition to the classical (nonresonant) term  $f_0$ , which is the Fourier transform of the electron density. The resonant contribution depends on the chemical nature of the scatterer and becomes substantial near its absorption edges. The associated specific properties are used in different ways to collect structural and spectroscopic information from crystals. Because of the local anisotropy of the outer shell unoccupied states, the resonant structure factor is a tensor that reflects the neighboring symmetry of the resonant atom. The anisotropy of this tensor leads to a number of phenomena such as x-ray dichroism, birefringence, or observation of “forbidden” reflections. The present Letter focuses on this last phenomenon.

It is well known that screw axis and glide plane symmetries lead to forbidden reflections. This general rule fails in the case of resonant scattering as a direct consequence of the anisotropy of the tensor structure factor [2,3]. This phenomenon has been observed in various crystals [2]. In particular, the polarization properties and the variation of the resonant diffracted intensity as a function of the rotation angle  $\varphi$  of the sample about the scattering vector  $\mathbf{Q}$  have been studied in several systems [1,4,5], allowing the determination of subtle structural data such as the localization of the resonant scatterer or its local anisotropy.

The observation of forbidden reflections has also been successfully used in chiral liquid crystals to determine the local periodic structure of several smectic- $C^*$  ( $\text{SmC}^*$ ) variants [6,7]. However, complete polarization studies have never been performed as a function of the rotation angle  $\varphi$ , essentially because of the usual helical precession of the chiral structure about the reciprocal vector  $\mathbf{Q}$  which amounts to averaging all of the tensor elements of the structure factor over  $\varphi$  [8]. We present in this Letter the

first complete polarization study performed on an achiral liquid crystal. The originality arises from the low dimensionality and the fluid nature of the mesophase. Unlike solid crystals, the limited alignment quality of the fluid sample has to be considered in data analyses.

Thermotropic liquid crystals (LCs) are complex fluids resulting from low-dimensional self-organization of organic molecules. In recent years, bent-core molecules have attracted a lot of attention for their rich and complex polymorphism, yet far from being well understood, and for unexpected physical properties such as ferroelectricity or the presence of twisted structures in achiral materials [9–11]. The description of the orientation of a bent-core molecule requires two parameters [11]. It is convenient to describe the molecule as a bow with two distinct axes: the string  $\mathbf{n}$  and the arrow  $\mathbf{b}$  [Fig. 1(a)]. The present study is devoted to a structural determination of the  $B_2$  phase for which four models have been proposed [Fig. 1(b)] corre-

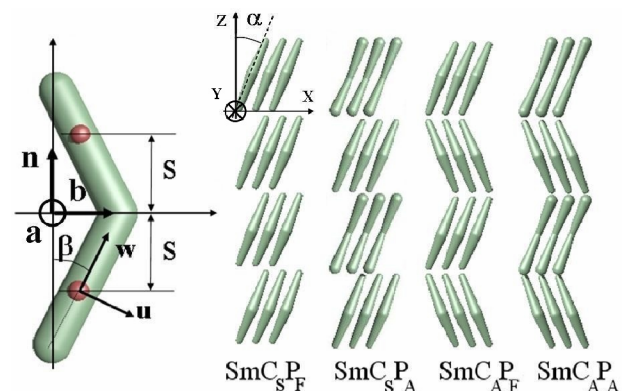


FIG. 1 (color online). (a) Left: Schematic view of a bent-core molecule as a bow. The orientation of the string and arrow are described by unit vectors  $\mathbf{n}$  and  $\mathbf{b}$ , respectively. (b) Right: Sketch of four possible arrangements in the  $B_2$  phase.  $\alpha$  is the  $\text{SmC}$ -like tilt of the string over the layer normal. The structures  $\text{SmC}_S P_F$  and  $\text{SmC}_A P_A$  are chiral, whereas  $\text{SmC}_S P_A$  and  $\text{SmC}_A P_F$  are racemic mixtures of chiral layers.

sponding to the four combinations of the SmC-like tilt of the string (synclinic or anticlinic) and of the arrow polarization (ferroelectric or antiferroelectric). The general notation  $\text{SmC}_{S \text{ or } A}P_{F \text{ or } A}$  summarizes these four states. Link *et al.* [12] have pointed out that the individual layers of the proposed structures are chiral (i.e., different from their mirror image) although the molecules are achiral.

The proposed  $B_2$  phase structures are formed by a regular stack of liquid layers of thickness  $d$  along a direction  $Z$ . The in-plane axes  $X$  (along the tilt direction) and  $Y$  (along the polarization arrow) complete the reference frame as shown in Fig. 1(b). The unit cell is one layer for the  $\text{SmC}_S P_F$  structure but two layers of opposite tilt and/or polarization for the other three. In reciprocal space, the basic wave vector component  $Q_z$  of the latter is then  $Q_0/2$ , with  $Q_0 = 2\pi/d$ . The corresponding half-order Bragg reflections are forbidden [glide plane ( $X, Z$ ) for the  $\text{SmC}_S P_A$  phase, ( $Y, Z$ ) for  $\text{SmC}_A P_F$ , and  $2_1$  screw axis for  $\text{SmC}_A P_A$ ]. The  $B_2$  phase studied in this work was investigated in an earlier work [13]. Intense resonant half-order peaks were detected, confirming a two-layer unit cell. This observation ruled out the  $\text{SmC}_S P_F$  structure, but no distinction could be made among the remaining three. Actually, electro-optical studies have evidenced an antiferroelectric behavior [12,14], and the important question reduces to distinguishing between the  $C_S P_A$  and  $C_A P_A$  structures.

Here we present a new study in which the polarization of the half-order resonant Bragg peaks is analyzed. We show that the polarization state of the diffracted beams depends strongly on the azimuthal rotation angle  $\varphi$  about the scattering vector  $\mathbf{Q}$ . We deduce the structure in the  $B_2$  phase.

The LC material  $(16\text{OTBB})_2$  represented in Fig. 2 is a bent-core molecule which exhibits the following phase sequence: isotropic (119 °C),  $B_2$  (108 °C), crystal [14]. The LC was spread in the  $B_2$  phase by rubbing along one direction on a  $12 \times 12 \text{ mm}^2$  glass substrate treated by deposition of a thin layer of surfactant (hexadecyl trimethyl ammonium bromide). This method is known to promote an excellent alignment of the layers parallel to the substrate [13]. The x-ray experiments were carried out at beam line X-19A of the National Synchrotron Light Source. A complete description of the three-circle diffraction set up was given in an earlier paper [7]. The LC sample was mounted on a fourth motorized  $\varphi$  rotation stage of axis  $Z$  (see inset in Fig. 2) fitted inside a two-stage oven allowing 20 mK resolution in temperature. The polarization of the diffracted beam was analyzed by a pyrolytic graphite crystal mounted on the two-theta arm. The beam size was set to  $500 \times 500 \mu\text{m}^2$ , and the vertical resolution  $\Delta Q_z$  was  $1.9 \times 10^{-3} \text{ \AA}^{-1}$ . A fluorescence energy scan was performed to tune the energy to the sulfur  $K$  edge at 2.473 keV.

The polarization of the Bragg peaks was recorded at  $T = 114.0 \text{ }^\circ\text{C}$  in the  $B_2$  phase by rotating the polarimeter about the direction  $\mathbf{k}_d$  of the diffracted beam. The rotation axis of the polarimeter was first carefully aligned along  $\mathbf{k}_d$

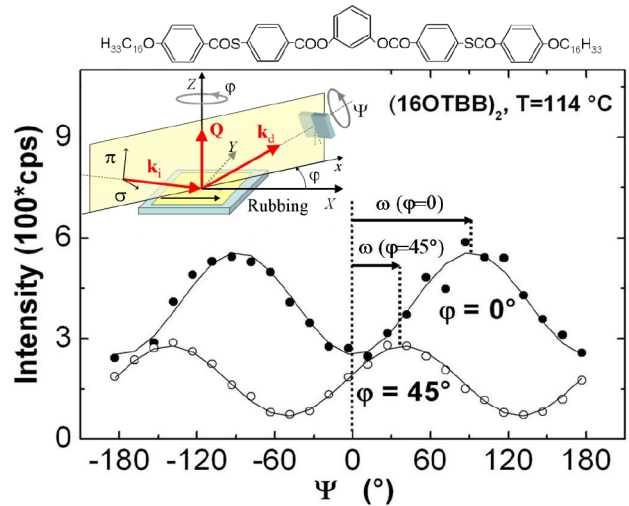


FIG. 2 (color online).  $\psi$  scans of the polarization analyzer for the 3/2 resonant peak. The intensity maxima, labeled by the angle  $\omega$ , indicate the rotation in polarization of the diffracted beam relative to the  $\sigma$  polarized incident beam.  $\varphi$  is the angle between the sample rubbing direction and the scattering plane (see inset). The molecule  $(16\text{OTBB})_2$  is shown on top.

through a couple of 0.5 mm pinhole apertures. In order to avoid a possible bias, a rocking scan of the graphite crystal was performed for each value of the polarimeter angle  $\psi$ . The linear  $\sigma$  polarization (i.e., perpendicular to the scattering plane) of the incident synchrotron beam and of the nonresonant 001 and 002 Bragg peaks were checked first, defining the origin of the polarimeter  $\psi = 0$  on a maximum of intensity. The extinction was almost complete (1.5%–3.5% residual intensity) and consistent with the imperfect Bragg angle of the graphite crystal ( $48.3^\circ$ ). The 3/2 region was then investigated, and a strong resolution limited resonant peak was found at  $Q/Q_0 = 3/2$  indicative of a

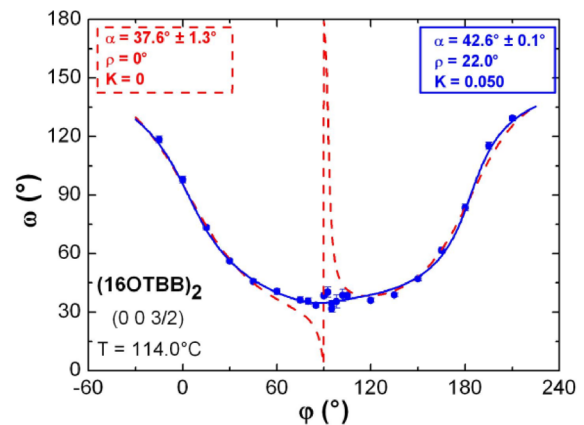


FIG. 3 (color online). Rotation  $\omega$  of the plane of polarization of the resonant 3/2 Bragg peak vs sample rotation  $\varphi$ . Dots are experimental points. The dashed line is a fit to the  $\text{SmC}_S P_A$  tensor model in the case of a perfect alignment. The solid line is a fit to the same model taking imperfect alignment into account (see text).

two-layer structure. Transverse theta scans across the Bragg peaks showed that the alignment of the layers was better than  $0.02^\circ$ . The layer thickness  $d = 2\pi/Q_0$  was  $42.0 \text{ \AA}$ .

The polarization direction of the  $3/2$  resonant peak is shown in Fig. 2 for two values of the sample azimuthal angle  $\varphi$ : (a)  $\varphi = 0$  defined as the beam parallel to the direction of rubbing (closed circles)—the polarization of the resonant Bragg peak is rotated by an angle  $\omega = 90^\circ$  relative to a  $\sigma$  polarized beam; (b)  $\varphi = 45^\circ$  (open circles)—the polarization of the Bragg peak is rotated by an angle  $\omega = 40^\circ$ . This shows that the polarization of the resonant peaks depends strongly on the azimuthal orientation of the sample. In order to check this dependence, the rotation of the polarization  $\omega$  was measured for different values of  $\varphi$ . The results displayed in Fig. 3 show that the polarization undergoes a giant rotation (from  $35^\circ$  to  $130^\circ$ ) upon rotating  $\varphi$ . The intensity of the

resonant Bragg peak decreases dramatically as  $\varphi$  approaches  $90^\circ$ .

We derive the form of the structure factor tensor from the symmetry elements of the molecule as follows: The resonant atoms occupy two equivalent sites at a distance  $S$  from the center of the molecule [Fig. 1(a)]. Following Ref. [8], we assume that the local polarizability tensor linked to each resonant atom is diagonal in a local principal frame ( $\mathbf{u}, \mathbf{v}, \mathbf{w}$ ) simply related to the arms of the bent-core molecule. We denote by  $F_u, F_v$ , and  $-(F_u + F_v)$  the three diagonal terms of this traceless tensor. It is straightforward to express the contribution of a single resonant site of a molecule in the molecular frame ( $\mathbf{a}, \mathbf{b}, \mathbf{n}$ ) via a rotation of angle  $\beta$  about  $\mathbf{v}$  and in the layer frame ( $X, Y, Z$ ) via a second rotation of angle  $\alpha$  about  $\mathbf{b}$ . Finally, the full contribution of a single layer is obtained by adding the contributions of the two sites with appropriate phase shift  $\exp(\pm i\phi)$ ; here  $\phi = Q_z S \cos\alpha$ . The polarizability of each layer of the  $B_2$  phase then reads:

$$\tilde{f}(\beta, \alpha) = \begin{bmatrix} 2(C + B\sin^2\alpha) & iA \sin\alpha & B \sin 2\alpha \\ iA \sin\alpha & -2(B + 2C) & iA \cos\alpha \\ B \sin 2\alpha & iA \cos\alpha & 2(C + B\cos^2\alpha) \end{bmatrix}, \quad (1)$$

with  $A = -(F_u + 2F_v)\sin 2\beta \sin\phi$ ,  $B = -[F_u(1 + \cos^2\beta) + F_v \cos 2\beta]\cos\phi$ , and  $C = F_u \cos\phi$ . Note that  $A, B$ , and  $C$  are complex numbers.

The tensor structure factor of the  $B_2$  phase is then constructed by summing up the layer contributions in a Fourier series over the whole stack, noting that the change of direction of the arrow and/or tilt corresponds simply to a change of sign of  $\beta$  and/or  $\alpha$ , respectively.

The four possible structures shown in Fig. 1 are generated by the four possible sign sequences of the angles  $\beta$  and  $\alpha$ . The coefficient  $A$  changes sign between neighboring layers in antiferroelectric structures, whereas  $\alpha$  changes sign in antclinic phases. Since we are interested in the contribution of the half-order resonant peaks, only those terms that change sign have to be considered. The diagonal terms in Eq. (1) contribute to the scattering at integer wave vectors and are buried in the nonresonant Bragg reflections. The relevant tensor components that contribute to the half-order resonant peaks for the three structures are then

$$\tilde{F}(\text{SmC}_S P_A) = \begin{bmatrix} 0 & iA \sin\alpha & 0 \\ iA \sin\alpha & 0 & iA \cos\alpha \\ 0 & iA \cos\alpha & 0 \end{bmatrix}, \quad (2a)$$

$$\tilde{F}(\text{SmC}_A P_F) = \begin{bmatrix} 0 & iA \sin\alpha & B \sin 2\alpha \\ iA \sin\alpha & 0 & 0 \\ B \sin 2\alpha & 0 & 0 \end{bmatrix}, \quad (2b)$$

$$\tilde{F}(\text{SmC}_A P_A) = \begin{bmatrix} 0 & 0 & B \sin 2\alpha \\ 0 & 0 & iA \cos\alpha \\ B \sin 2\alpha & iA \cos\alpha & 0 \end{bmatrix}. \quad (2c)$$

The tensor amplitudes have the form derived by Dmitrienko [3] for an ( $X, Z$ ) glide plane [Eq. (2a)], a ( $Y, Z$ ) glide plane [Eq. (2b)], and a  $2_1$  screw axis [Eq. (2c)]. This latter form is expected to produce a pure  $\pi$  polarization regardless of the azimuthal orientation  $\varphi$  [3], in clear contradiction with our observations. We rule it out and restrict our attention to the  $\text{SmC}_S P_A$  and  $\text{SmC}_A P_F$  cases.

The scattering amplitudes  $A_{\sigma\sigma} = \sigma_j \tilde{F}_{ij} \sigma_i$  and  $A_{\sigma\pi} = \pi_j \tilde{F}_{ij} \sigma_i$  along the polarization vectors  $\boldsymbol{\sigma}$  and  $\boldsymbol{\pi}$ , respectively, have been worked out in the general case by Dmitrienko [3]. The polarization states of the resonant reflections depend on the ratio of the two independent tensor elements in Eqs. (2a) and (2b). The case  $\text{SmC}_S P_A$  is remarkably simple since the ratio  $\tilde{F}_{XY}/\tilde{F}_{YZ} = \tan\alpha$  is real and independent of the unknown parameters  $F_u$  and  $F_v$ . Consequently, the polarization of the diffracted beam is linear along a direction that makes an angle  $\omega$  with the  $\sigma$  vector:

$$\tan\omega = \frac{A_{\sigma\pi}}{A_{\sigma\sigma}} = \frac{\cos\theta_B \cos\varphi / \tan\alpha - \sin\theta_B \cos 2\varphi}{\sin 2\varphi}, \quad (3)$$

in which  $\theta_B$  is the Bragg angle and  $\varphi$  is the angle between the glide plane direction  $X$  and the scattering plane. The data points are fitted to Eq. (3) in Fig. 3 (dashed line). The agreement is good with  $\alpha \approx 37^\circ$  except for the sharp variation around  $\varphi = \pi/2$ . At this point, we note that the model assumes a perfect orientation of the glide plane (i.e., the direction of the molecular tilt) in the plane of the layers. This is obviously not guaranteed and presumably not realistic in a biaxial fluid phase. If we consider instead that the

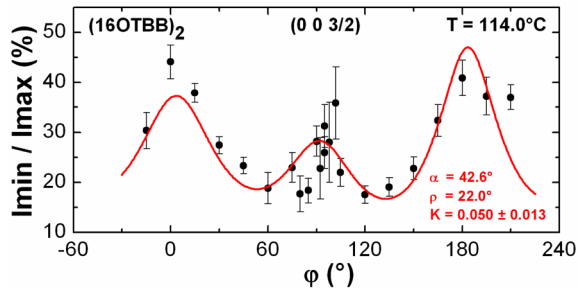


FIG. 4 (color online). Contrast ratio  $I_{\min}/I_{\max}$  of the polarimeter scans vs sample rotation angle  $\varphi$ . The line is a fit taking imperfect alignment of a  $\text{SmC}_S P_A$  structure into account (see text).

direction of tilt is distributed with some angular spread about an average direction imposed by the rubbing action, the agreement becomes excellent. The solid curve in Fig. 3 is a fit to the tensor model with an *ad hoc* Gaussian distribution  $\mathcal{P}(\varphi)$  of the in-plane orientation of the molecular tilt proportional to  $[\exp(-\varphi^2/2\rho^2) + K]$ , with  $\rho = 22.0^\circ$  and  $K = 0.05$ . The best value of the tilt angle  $\alpha$  is  $42.6 \pm 0.1^\circ$ . Combined with the layer spacing  $d$ , it yields an end-to-end molecular length of 62 Å, compatible with geometrical molecular models.

Figure 2 shows, however, that the minima of intensity of the polarimeter scans are not zero as they should be for a pure linear polarization. The experimental values of the ratio  $I_{\min}/I_{\max}$  of the minima to the maxima are plotted against  $\varphi$  in Fig. 4. It is easy to check that the imperfect in-plane alignment introduced above can simply explain this lack of extinction. The line in Fig. 4 is a fit to the contrast ratio calculated with the same in-plane angular distribution  $\mathcal{P}(\varphi)$ . The agreement is reasonably good.

Our experimental data are hence fully consistent with the  $\text{SmC}_S P_A$  structure of the  $B_2$  phase with one adjustable structural parameter, namely, the tilt angle  $\alpha$  when an angular distribution of the in-plane orientation of the molecular tilt is taken into account. Note that  $\omega(\varphi)$  differs from  $\omega(\varphi + \pi)$  which indicates that the sense of rubbing is relevant and gives access to the sign of  $\alpha$ . We found that the best fit corresponds to a tilt of the molecules along the direction of rubbing.

Although not consistent with the antiferroelectric response of the  $B_2$  phase, the case of the  $\text{SmC}_A P_F$  structure can be discussed for completeness. Since the ratio  $\tilde{F}_{XY}/\tilde{F}_{XZ} = iA \sin\alpha/B \sin 2\alpha$  in Eq. (2b) is complex, the polarization of the resonant peaks is expected to be elliptical. Numerical simulations show that the imaginary part  $\text{Im}(\tilde{F}_{XY}/\tilde{F}_{XZ})$  that controls the ellipticity increases naturally the contrast ratio  $I_{\min}/I_{\max}$  but does not affect very much the  $\omega$  vs  $\varphi$  curve (in this case,  $\omega$  would be the angle

between the direction of the long axis of the elliptical wave and the polarization vector  $\sigma$ ). Consequently, an in-plane angular disorientation would have to be invoked again to fit our data (i.e., to smooth out the sharp variation around  $\varphi = \pi/2$ ). Eventually, fits equivalent to those shown in Figs. 3 and 4 are obtained for a set of combinations of  $\rho$ ,  $K$ , and  $\text{Im}(\tilde{F}_{XY}/\tilde{F}_{XZ})$ . Strictly speaking, our experimental data are thus compatible with the two structures  $\text{SmC}_S P_A$  and  $\text{SmC}_A P_F$  and cannot distinguish between them. However, the nice coincidence between the ratio of the tensor elements  $\tilde{F}_{XY}/\tilde{F}_{XZ}$  and  $\tan\alpha$  with a reasonable value of  $\alpha$  (which comes out naturally from the  $\text{SmC}_S P_A$  model) would be fortuitous in the  $\text{SmC}_A P_F$  case, which seems unlikely.

In conclusion, the full tensor properties of resonant scattering of x rays have been investigated for the first time on a complex fluid system. We found that the polarization properties of the resonant Bragg peaks can be fully interpreted within existing models [3] if a distribution of sample alignment is taken into account. As a result, the validity of the  $\text{SmC}_S P_A$  model of an antiferroelectric  $B_2$  phase is confirmed by structural studies for the first time.

Research at the NSLS, BNL, was supported in part by the U.S. Department of Energy, Division of Materials Sciences and Division of Chemical Sciences, under Contract No. DE-AC02-98Ch10886. The research was also supported in part by the donors of the Petroleum Research Fund, administered by the American Chemistry Society. P.F. acknowledges support from the Portuguese Foundation for Science and Technology.

- 
- [1] J.L. Hodeau *et al.*, Chem. Rev. **101**, 1843 (2001).
  - [2] D.H. Templeton and L.K. Templeton, Acta Crystallogr. Sect. A **41**, 133 (1985).
  - [3] V.E. Dmitrienko, Acta Crystallogr. Sect. A **39**, 29 (1983).
  - [4] A. Kirfel and A. Petcov, Acta Crystallogr. Sect. A **48**, 247 (1992).
  - [5] D.H. Templeton and L.K. Templeton, Acta Crystallogr. Sect. A **42**, 478 (1986); M. Fabrizio, M. Altarelli, and M. Benfatto, Phys. Rev. Lett. **80**, 3400 (1998).
  - [6] P. Mach *et al.*, Phys. Rev. Lett. **81**, 1015 (1998).
  - [7] P. Mach *et al.*, Phys. Rev. E **60**, 6793 (1999).
  - [8] A.-M. Levelut and B. Pansu, Phys. Rev. E **60**, 6803 (1999).
  - [9] T. Niori, T. Sekine, J. Watanabe, T. Furukawa, and H. Takezoe, J. Mater. Chem. **6**, 1231 (1996).
  - [10] G. Pelzl, S. Diele, and W. Weissflog, Adv. Mater. **11**, 707 (1999).
  - [11] H.R. Brand, P.E. Cladis, and H. Pleiner, Eur. Phys. J. B **6**, 347 (1998).
  - [12] D. Link *et al.*, Science **278**, 1924 (1997).
  - [13] A. Cady *et al.*, Liq. Cryst. **29**, 1101 (2002).
  - [14] J.C. Rouillon *et al.*, J. Mater. Chem. **11**, 2946 (2001).